SUPPLEMENTAL INFORMATION

Local Reaction Environment for Selective Electroreduction of Carbon Monoxide

Ming Ma,[†,‡,*] Wanyu Deng,[‡] Aoni Xu,[‡] Degenhart Hochfilzer,[‡] Yu Qiao,[‡] Karen Chan,[‡,*] Ib Chorkendorff[‡] and Brian Seger[‡,*]

[†]School of Chemical Engineering and Technology, Xi'an Jiaotong University, Xi'an 710049, People's Republic of China

[‡]Surface Physics and Catalysis (Surfcat) Section, Department of Physics, Technical University of Denmark, 2800 Kgs Lyngby, Denmark

*Author to whom correspondence should be addressed.

E-mail address: mingma@xjtu.edu.cn; kchan@fysik.dtu.dk; brse@fysik.dtu.dk

Tel.: +45 45253174

Materials

In this work, potassium bicarbonate ($KHCO_3$, ≥99.95%) and potassium hydroxide hydrate ($NaOH \cdot xH_2O$, 99.995%, Suprapur®) purchased from Sigma Aldrich were used without further purification. Anion exchange membrane (AEM, Fumasep FAA-3-PK-75) and gas-diffusion electrode (GDE, Sigracet 39 BC), which were used in our flow electrolyzers, were purchased from Fuel Cell Store. Iridium dioxide (IrO_2) purchased from Dioxide Materials was employed as an anode in flow electrolyzers for high-rate CO reduction.

Catalysts characterizaton

Via direct current magnetron sputtering (50 W), Cu catalyst layers were synthesized on microporous layer of gas-diffusion electrodes. By controlling the deposition time, the constant thickness of the Cu layers can be achieved.

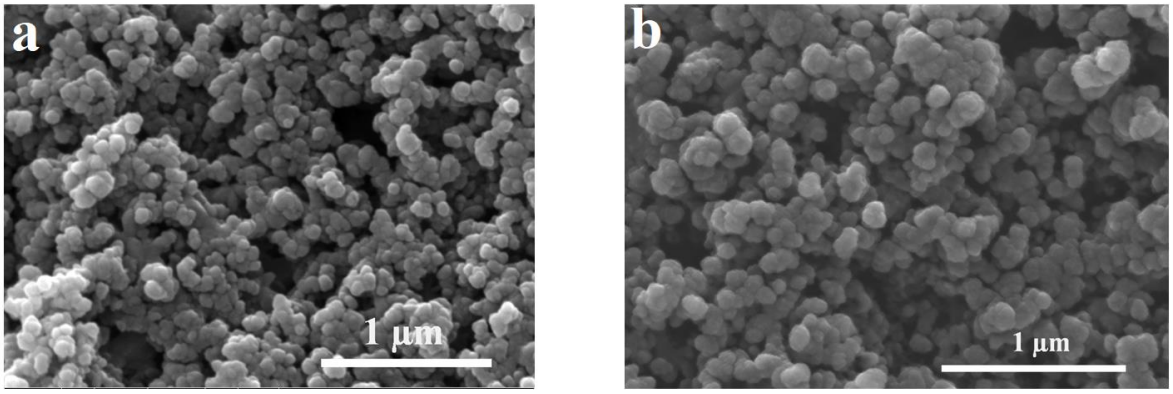

Figure S1. Cu catalysts coated on microporous carbon layers of gas-diffusion electrodes before (a) and after (b) CO reduction in 1 M KOH.

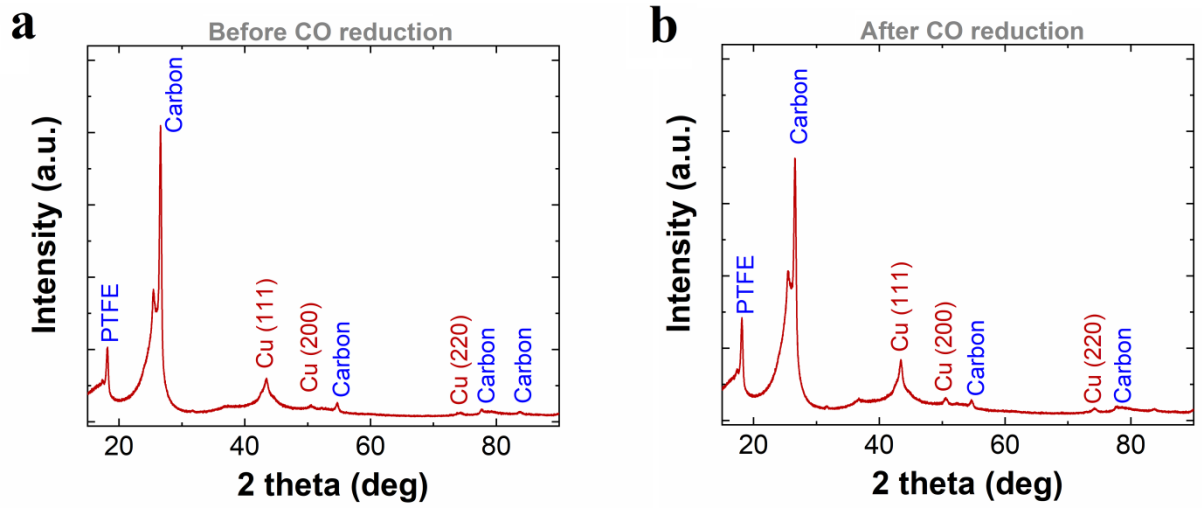

Figure S2. XRD patterns of Cu coated on a gas-diffusion electrode (Sigracet 39 BC) before (a) and after (b) CO reduction in 1 M KOH. XRD measurements were carried out using Cu Kα radiation.

CO_2 reduction performance

The electrocatalytic CO conversion was implemented in a Teflon three-chamber flow electrolyzer made from Teflon at ambient temperature and pressure at various pH electrolyte. The catholyte and anolyte flow compartments were separated by an ion-selective membrane. The catholyte and anolyte reservoirs filled with 50 ml electrolyte were circulated, as shown in Figure S3.

A constant CO flowrate of 45 ml/min was purged into gas compartment, and a part of CO diffused to the catalyst surface in electrolyte for CO conversion, forming various gaseous and liquid products. The gaseous products mixed with unreacted CO were vented out of the electrolyzer, injecting into the gas-sampling loop of a gas chromatography (PerkinElmer, Clarus® 590) for identification and quantification. For accurate calculation of faradaic efficiencies for gaseous products, the volumetric flowrate of gas outlet (gas mixture)

after electrolyzers was monitored by flow meter in the course of CO reduction electrolysis (Figure S3). It should be noted that the average catalytic selectivity for gaseous products over ~3 h CO electrolysis was employed in this study. In addition, the liquid-phase products that were collected after CO reduction electrolysis were analyzed via a high performance liquid chromatography (HPLC, Agilent 1200 series), which is equipped with an Aminex HPX-87H column (Bio-Rad) that was maintained at 50 °C, a diode array detector (DAD) and a refractive index detector (RID).

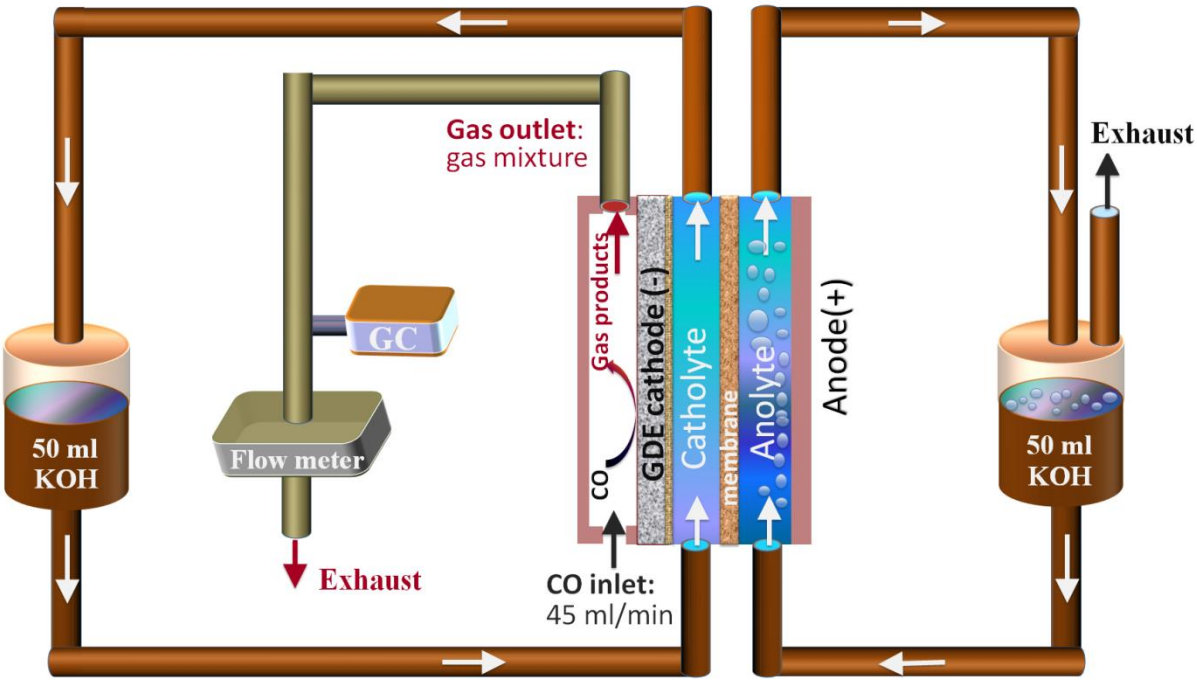

Figure S3. Schematic illustration of GDE-type flow electrolyzers for electrochemical CO reduction.

Table S1. The experimentally measured gas flow out of the electrolyzers for high-rate CO reduction as a function of current density in 1 M $KHCO_3$ (inlet CO flowrate is 45 ml/min).

J (mA/cm^2)	$\emptyset_{outlet}$(ml/min)	Standard Deviation
100	44.83	0.07
150	44.55	0.1
200	44.67	0.16
250	45.94	0.13
300	46.0	0.1

Theoretical gas flow out of electrolyzers for high-rate CO reduction

In the electrocatalytic CO reduction, CO flowrate that is converted into one certain product can be calculated as:

$$\emptyset_{CO\ to\ x} = \left(n_c \times \frac{Q_{tot} \times FE_x}{n_e F}\right) \times \frac{RT}{P_o} \quad (S1)$$

where Q_{tot} and FE_x are charge passed through the cathode and faradaic efficiency for one certain product (x), respectively. n_c and n_e are the number of CO and number of electron required for generating one molecule of certain product. *F* is Faradaic constant, *R* is ideal gas constant, T is absolute temperature, and P_o is ambient pressure. From the total current (I_{tot}) and the electrolysis time (t), we can get the equation: $Q_{tot} = I_{tot} \times t$.

The consumed CO flowrate that is converted into all gaseous products (C_2H_4 and CH_4) in CO reduction can be expressed as:

$$\emptyset_{CO\ to\ gas} = \emptyset_{CO\ to\ C_2H_4} + \emptyset_{CO\ to\ CH_4} \quad (S2)$$

where $\emptyset_{CO\ to\ C_2H_4}$ is the consumed CO flowrate that is relectrochemically reduced to C_2H_4, and $\emptyset_{CO\ to\ CH_4}$ is the reacted CO flowrate that is converted into CH_4 in CO reduction. The total consumed CO flowrate that is electrochemically reduced to all the detected liquid-phase products can be written as:

$$\emptyset_{CO\ to\ liquid} = \emptyset_{CO\ to\ acetate} + \emptyset_{CO\ to\ ethanol} + \emptyset_{CO\ to\ propanol} + \emptyset_{CO\ to\ allyl\ alcohol} + \emptyset_{CO\ to\ acetaldehyde} \quad (S3)$$

where $\emptyset_{CO\ to\ acetate}$ and $\emptyset_{CO\ to\ ethanol}$ are the CO flowrates that are electrochemically converted into the major liquid products of acetate and ethanol in the electrocatalytic reduction of CO, respectively. $\emptyset_{CO\ to\ propanol}$, $\emptyset_{CO\ to\ allyl\ alcohol}$ and $\emptyset_{CO\ to\ acetaldehyde}$ are the

consumed CO flow that are responsible for the minor products of n-propanol, allyl alcohol and acetaldehyde, respectively. Based on equations S2 and S3, the residual unreacted CO flowrate out of gas compartment of the electrolyzers can be calculated as:

$$\emptyset_{residual\ \mathrm{CO}} = \emptyset_{inlet\ \mathrm{CO}} - (\emptyset_{CO\ to\ gas} + \emptyset_{CO\ to\ liquid}) \quad \text{(S4)}$$

where $\emptyset_{inlet\ CO}$ is the CO inlet flowrate that is fed into the gas chamber. It should be noted that $\emptyset_{inlet\ CO}$ is accurately controlled at 45 ml/min by mass flow controller. We can get the flowrate out of the electrolyzers in CO reduction:

$$\emptyset_{outlet} = \emptyset_{residual\ CO} + \emptyset_{CH_4} + \emptyset_{C_2H_4} + \emptyset_{H_2} \quad \text{(S5)}$$

where $\emptyset_{CH_4}$, $\emptyset_{C_2H_4}$ and $\emptyset_{H_2}$ is the flow of CH_4 , C_2H_4 and H_2 in CO reduction. Thus, we can get the theoretical gas flow out of the electrolyzers in high-rate CO reduction in Table S2, which is consistent with our experimental observation of that no significant discrepancy in the flowrate between gas inlet and outlet in CO reduction. Even there was no significant variation in the flow between gas inlet and outlet, we still used the measured gas outlet flowrate for the calculation of faradaic efficiency.

Table S2. Theoretical gas flow out of the electrolyzers for high-rate CO reduction as a function of current density in 1 M $KHCO_3$ (inlet CO flowrate is 45 ml/min).

J (mA/cm^2)	$\emptyset_{CH_4}$ (ml/min)	$\emptyset_{C_2H_4}$ (ml/min)	$\emptyset_{H_2}$ (ml/min)	$\emptyset_{residual\ CO}$ (ml/min)	$\emptyset_{outlet}$(ml/min)
100	0.078	0.009	0.084	44.670	44.841
150	0.103	0.020	0.157	44.455	44.735
200	0.113	0.042	0.237	44.260	44.652
250	0.115	0.072	0.348	44.134	44.669
300	0.119	0.054	0.690	44.127	44.990

High local pH near the cathode in CO reduction

In the electrocatalytic CO reduction process, CO and H_2O can be electrocatalytically reduced to numerous gas and liquid products on the surface of the Cu catalyst in electrolytes. The gaseous products such as C_2H_4 and CH_4 are formed according to the following reactions[1]:

$$2CO + 6H_2O + 8e^- \rightarrow C_2H_4 + 8OH^- \quad \text{(S6)}$$

$$CO + 5H_2O + 6e^- \rightarrow CH_4 + 6OH^- \quad \text{(S7)}$$

In addition to gaseous products, liquid products including acetate, ethanol and n-propanol also could be generated in electrocatalytic reduction of CO, as follows:

$$2CO + 3H_2O + 4e^- \rightarrow CH_3COO^- + 3OH^- \quad \text{(S8)}$$

$$2CO + 7H_2O + 8e^- \rightarrow CH_3CH_2OH + 8OH^- \quad \text{(S9)}$$

$$3CO + 10H_2O + 12e^- \rightarrow C_3H_7OH + 12OH^- \quad \text{(S10)}$$

It is generally known that H_2 evolution is an unavoidable competing reaction with CO reduction in flow electrolyzers. The electroreduction of H_2O to H_2 is based on the below reaction[2]:

$$2H_2O + 2e^- \rightarrow H_2 + 2OH^- \quad \text{(S11)}$$

A large amount of OH^- ions can be generated at the cathodic GDE/catholyte interface via the aforementioned cathodic reactions [equations S(6-11)], thus leading to a much higher pH locally in the vicinity of the cathodic GDE surface in comparison with that of the bulk electrolyte.

CO_2 capture via high local pH

During CO_2 reduction in flow electrolyzers, OH^- ions can be generated by the cathodic reactoins as below:

$$xCO_2 + yH_2O + ne^- \rightarrow product + nOH^- \quad \text{(S12)}$$

Thus, the total CO_2 consumption in the CO_2 electrolysis can be divided into two parts: (i) the consumed CO_2 that is converted into products, and (ii) CO_2 from the gas chamber of the electrolyzers reacts with OH^- ions produced at the cathode/electrolyte interface in the CO_2 elecrolysis, forming carbonate (*i.e.* captured CO_2 via reaction with OH^-).[3]

Detailed CO_2 capture reactions near the cathodic GDE surface can be expressed as:

$$OH^- + CO_2 \leftrightarrow HCO_3^- \quad \text{(pKa=7.8*)} \quad \text{(S13)}$$

$$OH^- + HCO_3^- \leftrightarrow CO_3^{2-} + H_2O \quad \text{(pKa=10.3)} \quad \text{(S14)}$$

* This is at a CO_2 partial pressure of 1 bar in 1 M HCO_3^-.[3]

It should be noted that CO_2 capture rate is also correlated with the active GDE surface area used in flow electrolyzers and mass transport properties that may be influenced by the type of GDEs, reactor design, catholyte flow, etc. In this work, all these parameters were identical for all the tests.

CO_2 capture rate calculation as a function of current density

The CO_2 capture rate (i.e consumed CO_2 flowrate) via the reaction with OH^- in the vicinity of the cathodic GDE surface in flow electrolzyers can be calculated as:

$$\emptyset_{OH^-} = \emptyset_{inlet\ CO_2} - (\emptyset_{residual\ CO_2} + \emptyset_{CO_2\ to\ gas} + \emptyset_{CO_2\ to\ liquid}) \quad (S15)$$

where $\emptyset_{inlet\ CO_2}$ and $\emptyset_{residual\ CO_2}$ are the inlet flowrate of CO_2 that was purged into the gas compartment and the residual unreacted CO_2 flowrate in the gas outlet out of gas compartment, respectively. $\emptyset_{CO_2\ to\ gas}$ is the consumed CO_2 flowrate that is converted into all gaseous products (CO, C_2H_4 and CH_4) in CO_2 reduction. $\emptyset_{CO_2\ to\ liquid}$ is the consumed CO_2 flowrate that is electrochemically reduced to liquid-phase products.

In the above equation, $\emptyset_{inlet\ CO_2}$ can be accurately controlled by mass flow controller. The $\emptyset_{CO_2\ to\ gas}$ can be expressed as:

$$\emptyset_{CO_2\ to\ gas} = \emptyset_{CO} + \emptyset_{CH_4} + 2\emptyset_{C_2H_4} \quad (S16)$$

where $\emptyset_{CO}$, $\emptyset_{CH_4}$ and $\emptyset_{C_2H_4}$ are the gas flowrate for CO, CH_4 and C_2H_4 produced in the electrocatalytic reduction of CO_2.

$\emptyset_{CO_2\ to\ liquid}$ can be writen as:

$$\emptyset_{CO_2\ to\ liquid} = \emptyset_{C_1} + \emptyset_{C_2} + \emptyset_{C_3} \quad (S17)$$

where $\emptyset_{C_1}$, $\emptyset_{C_2}$, and $\emptyset_{C_3}$ are the consumed CO_2 flowrate for generating C_1, C_2 and C_3 liquid products, respectively.

$\emptyset_{residual\ CO_2}$ can be easily obtained as below:

$$\emptyset_{residual\ CO_2} = \emptyset_{outlet} - (\emptyset_{CO} + \emptyset_{CH_4} + \emptyset_{C_2H_4} + \emptyset_{H_2}) \quad (S18)$$

where $\emptyset_{outlet}$ is the detected gas flowrate out of the electrolyzers in the course of CO_2 electrolysis using a volumetric flow meter.[3,4] $\emptyset_{H_2}$ is H_2 flowrate formed in the reduction of CO_2.

According to the above equation S15-S18, CO_2 capture rate can be obtained as shown in Table S3.

Table S3. CO_2 capture rate as a function of current density in 1 M $KHCO_3$ (most of the data were adapted based on our previous work[3]).

J (mA/cm^2)	$\emptyset_{CO_2\ to\ gas}$ (ml/min)	$\emptyset_{CO_2\ to\ liquid}$ (ml/min)	$\emptyset_{OH^-}$ (ml/min)
100	0.391	0.149	1.072
150	0.749	0.267	1.9292
200	0.922	0.371	2.9011
250	1.169	0.4226	3.6732
300	1.379	0.516	4.4885

CO_2 capture rate calculation as a function of pH

For linking the capture ability of CO_2 with OH^- concentration (*i.e.* pH), CO_2 capture rate in the form of CO_3^{2-} was detected in various concentrations of KOH electrolyte at the open-circuit potential under an inlet flowrate of 45 ml/min. Figure S4 shows that CO_2 capture rate as a function of OH^- concentration. In addition, CO_2 capture rate as a function of pH (Figure S5) was also adapted based on Figure S4. A comparison of the CO_2 capture rate during CO_2 reduction at different current densities and the CO_2 capture rate at open-circuit potential in various pH electrolytes is shown in Figure S6. The dash lines in Figure S6 present the equivalent CO_2 capture rate in the form of CO_3^{2-} between CO_2 reduction at various current densities and open-circuit potential in various pH electrolytes, which enables us to determine the local pH values for CO reduction at various current densities.

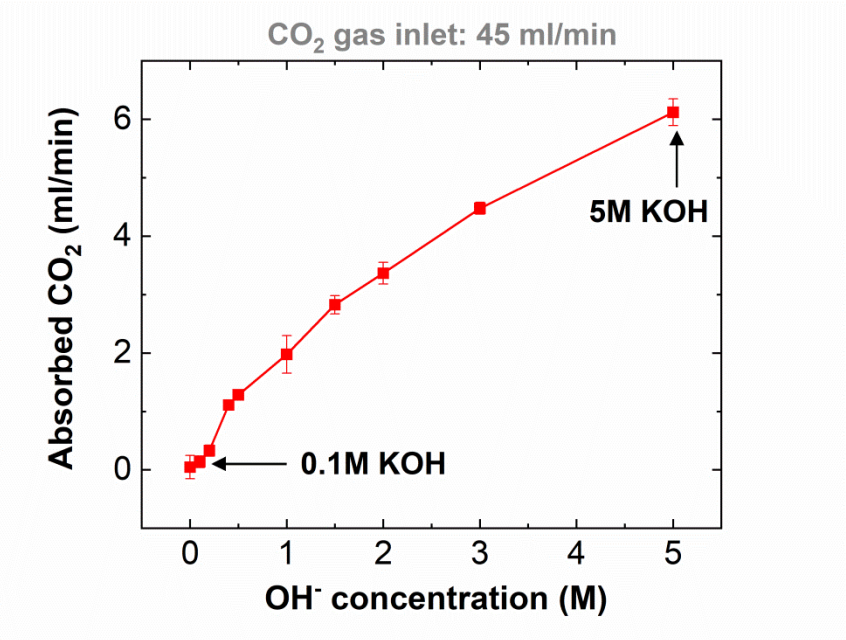

Figure S4. CO_2 capture rate measured in various concentrations of KOH electrolyte at the open-circuit potential under an inlet flowrate of 45 ml/min.

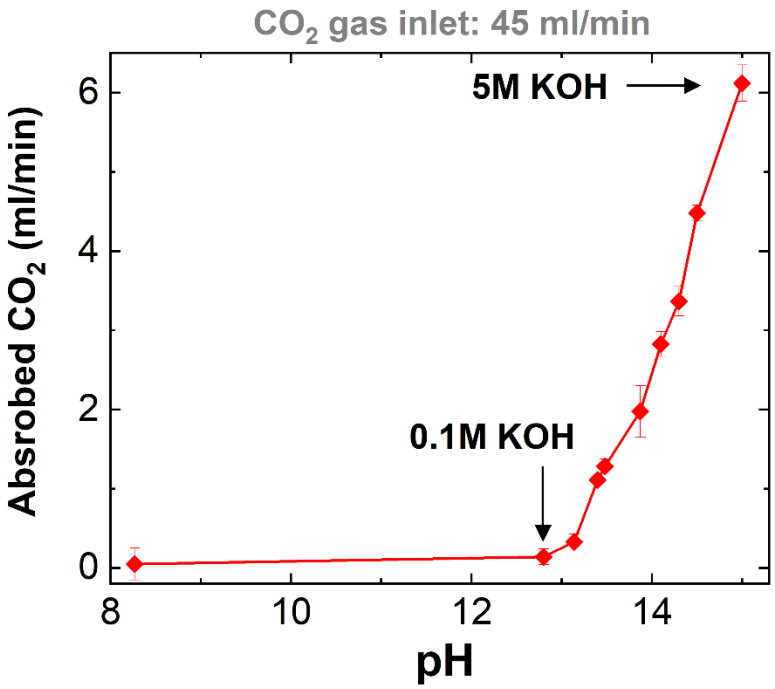

Figure S5. Measured CO_2 capture rate as a function of pH without electrolysis.

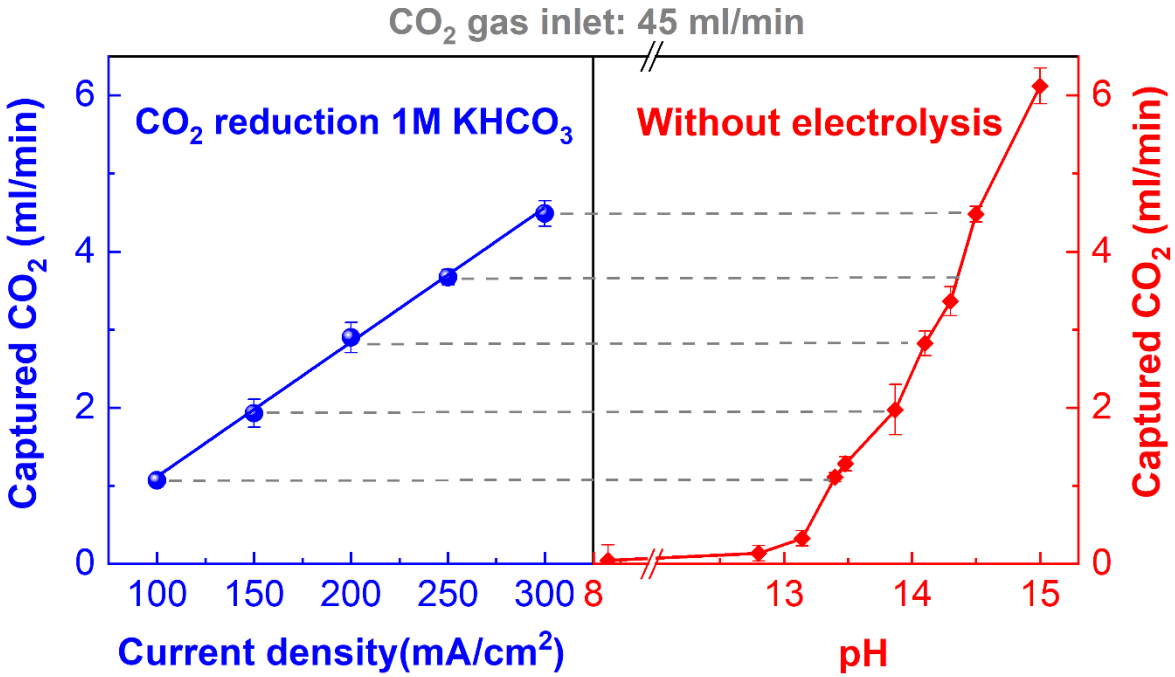

Figure S6. A comparison of CO_2 capture rate for CO_2 reduciton at various current densities and for open-circuit potential at various pH electrolyte.

Table S4. OH^- concentration near the cathodic GDE/electrolyte interface during CO reduction electrolysis as a function of current density in 1 M $KHCO_3$ (local pH was determined by experimental method mentioned in this work).

J (mA/cm^2)	$OH^- concentration$ (M)	Local pH
100	~0.4	~13.4
150	~1	~13.9
200	~1.5	~14.1
250	~2	~14.3
300	~3	~14.5

Table S5. OH^- concentration near the cathodic GDE/electrolyte interface during CO reduction electrolysis at 100 mA/cm^2 in 1 M $KHCO_3$ 0.5 M KOH, 1 M KOH and 2 M KOH, respectively (local OH^- concentration was determined by experimental method mentioned in this work).

Electrolyte	$OH^- concentration$ (M)
1 M $KHCO_3$	~0.4
0.5 M KOH	~0.9
1 M KOH	~1.5
2 M KOH	~2.4

Boundary layer thickness Test

For an electrochemical cell, the thickness of hydrodynamic boundary layer could be quantified through the measurement of the diffusion-limited current of ferricyanide reduction[5]:

$$Fe(CN)_6^{3-} + e^- \rightarrow Fe(CN)_6^{4-} \quad \text{(S19)}$$

This reduction has the electrochemical reversibility, which means that the reduction of ferricyanide is facile such that the observed rate is limited only by mass transfer regardless of the applied overpotential. Thus, ferricyanide reduction is an ideal reaction to determine the hydrodynamic boundary layer thickness. The total ferricyanide concentration should be minimized when performing this test, and the supporting electrolyte should be equivalent to that of the utilization during CO reduction. Thereby, the fluid properties of the electrolytes used for the quantification of the hydrodynamic boundary layer thickness could accurately reflect those of the solutions typically utilized for measuring the electrocatalytic activity. Furthermore, carbon paper without Cu catalyst should be utilized to conduct the measurement to avoid Galvanic corrosion processes in which ferricyanide is the oxidizing agent.

Figure S7a depicts cyclic voltammograms measured in electrolytes (0.5 M $KHCO_3$, 0.5 M KOH, 1 M KOH, and 2 M KOH) with the addition of 10 mM $K_3Fe(CN)_6$. There is a potential window of ~300 mV where the observed Faradaic current can be attributed entirely to ferricyanide reduction from -0.4 V to -0.1 V. Furthermore, the observed rate of ferricyanide reduction is independent of the applied voltage, which is a result of its electrochemical reversibility, as previously mentioned. Thus, the steady state diffusion-limited current density associated with ferricyanide reduction can be measured and utilized to calculate the average hydrodynamic boundary layer thickness at the cathode surface using Fick's law:

$$\delta_{BL} = \frac{F \times D_{Fe(CN)_6^{3-}} \times C_{Fe(CN)_6^{3-}}}{j} \quad (S20)$$

where δ_{BL} is the boundary layer of the flow cell. F is Faraday constant and equals to 96485 C/mol; $D_{Fe(CN)_6^{3-}}$ equals to 7.26 × 10^{-6} cm^2/s.[6] $C_{Fe(CN)_6^{3-}}$ is the concentration of $Fe(CN)_6^{3-}$ and equals to 10 mM; j is Faradaic current density of Ferricyanide reduction reaction.

As shown in Figure S7b, the steady state current density associated with ferricyanide reduction. Base on this method the boundary layers in 0.5 M $KHCO_3$, 0.5 M KOH, 1 M KOH, and 2 M KOH electrolyte are 64.9, 70.0, 64.3, and 70.0 μm, respectively.

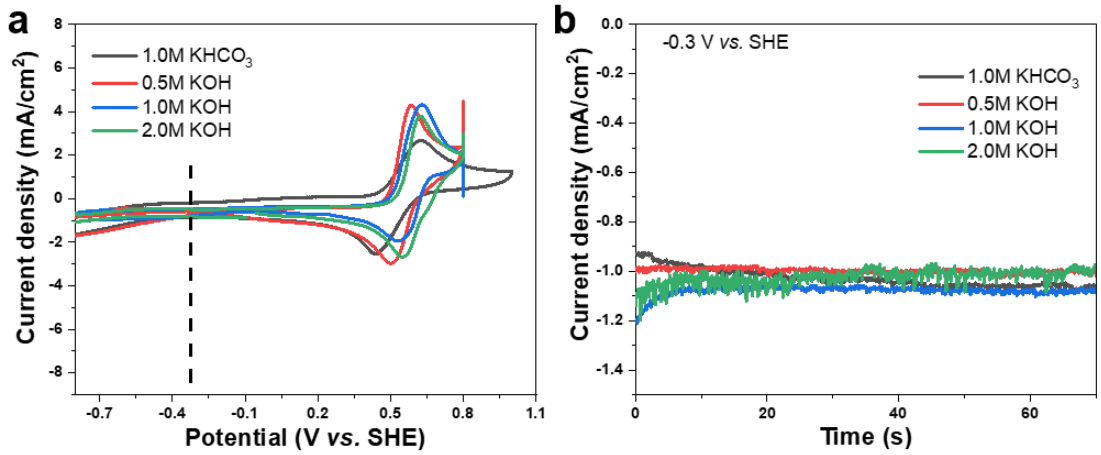

Figure S7. (a) Cyclic voltammograms obtained in the different electrolytes with the addition of 10 mM $K_3Fe(CN)_6$. The dotted black line indicates the potential used in the subsequent chronoamperometry experiments. (b) Chronoamperometry experiments utilized to measure the diffusion-limited current density of ferricyanide reduction under a series of different hydrodynamic conditions.

Details of coupled microkinetic-mass transport simulation

The model of CO-to-Acetate has been simulated in the previous work.[7] Here we reproduce below a summary of the details of ref.7.

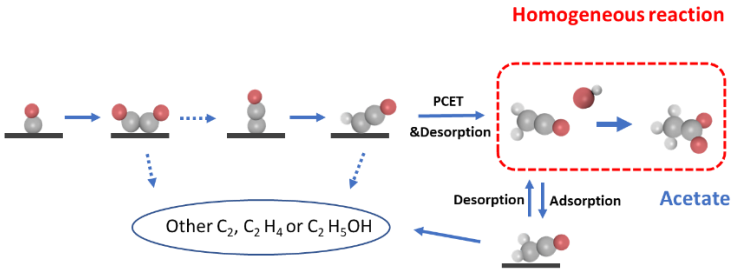

Scheme S1. Simulation reaction pathway of CO_2 reduction on Cu (acetate formation is a homogenous reaction).

The reaction S21 is a selectivity-dependent step for acetate (CH_3COO^-)

$$H_2CCO + OH^- \rightleftharpoons CH_3COO^- \qquad (S21)$$

This reaction is a homogeneous reaction whose rate is dependent on the rate constant[8] of $5.26 \cdot 10^4\ (mol \cdot s)^{-1}$ and the concentration of H_2CCO and OH^-. Meanwhile, H_2CCO is produced on Cu surface from CO via a microkinetic model with DFT calculations, while the concentration of H_2CCO and OH^- in the vicinity of Cu is dependent on mass transport.

Mass transport model as below:

The transport of electrolyte is solved via a 1-D model employing Poisson-Nernst-Planck equation with a boundary thickness of 70 μm.

$$\frac{dc}{dt} = -\frac{d}{dx}\left[D\frac{dc}{dx} - D\frac{z_i}{k_B T}c\left(\frac{d\phi}{dx}\right)\right] \qquad (S22)$$

$$\frac{d}{dx}\left(\epsilon\frac{d\phi}{dx}\right) = -\sum_i z_i c_i \qquad (S23)$$

where c is the concentration, D is diffusion coefficient, z_i is the charge of species i, ϕ is the potential, x is the distance, t is the time, k_B is the Boltzmann constant and T is the absolute temperature. In Eq. S23, ϵ is the permittivity of solvent. To solve these equations, we set up the Neumann boundary conditions at electrode side and Dirichlet boundary conditions at solution side:

x=0 (electrode surface):

$$f(CO) = f(H_2CCO) + f(otherC_2) \quad (S24)$$

$$f(OH^-) = 4 \cdot f(H_2CCO) + 8 \cdot f(otherC_2) \quad (S25)$$

$$f(Ac^-) = \int_0^\infty [H_2CCO]\,[OH^-] k_{sol} dx \quad (S26)$$

Here, f is species flux, which could be related to current density at electrode surface (obtained from microkinetic model), $f(CO) = \frac{j(CO)}{2F}$, F is Faraday constant.

At x=70 μm (solution side):

$$c_i = c_i^{bulk} \quad (S27)$$

$$\phi = 0 \quad (S28)$$

After involving reaction (equation S21) into simulation model, the transport of CO, OH^- and H_2CCO follow as:

$$\frac{d[CO]}{dt} = -D_{CO} \frac{d^2[CO]}{dx^2} \quad (S29)$$

$$\frac{d[OH^-]}{dt} = -2 \cdot D_{OH^-} \frac{d^2[OH^-]}{dx^2} - k_{sol}[OH^-][H_2CCO] \quad (S30)$$

$$\frac{d[H_2CCO]}{dt} = -D_{H_2CCO} \frac{d^2[H_2CCO]}{dx^2} - k_{sol}[OH^-][H_2CCO] \quad (S31)$$

where the k_{sol} is the rate constant of the reaction S21, which is $5.26 \cdot 10^4\ (mol \cdot s)^{-1}$. For diffusion coefficients we used $D_{CO} = 20.3 \cdot 10^{-10} m^2/s$, $D_{OH^-} = 52.7 \cdot 10^{-10} m^2/s$, $D_{H_2CCO} = 14.0 \cdot 10^{-10} m^2/s$.[9,10]

In addition, it has demonstrated that pH calculation for highly concentrated alkaline solutions is very complicated, thus the calculation of pH value from OH^- concentration in this work was based on the guidance in ref. 11.

Microkinetic model:

Coupled to the 1D mass transport model was the microkinetic model simulated the CO2RR reactions on Cu surface following the reaction pathway as below,

$CO + * + e^- \rightarrow *CO$

$2*CO + 3\ H_2O^+ + 3e^- \rightarrow *HCCO + 3OH^-$

$*HCCO + H_2O^+ + e^- \rightarrow H_2CCO_{(aq)} + OH^-$

$H_2CCO_{(aq)} \rightleftharpoons *H_2CCO$

$H_2CCO_{(aq)} + OH^- \rightleftharpoons CH_3COO^-$ (Acetate)

$*H_2CCO \rightarrow$ other C_{2+}

This reaction network was solved with the Markovian master equation, which describes the coverage θ arising from both forward and backward reactions,

$$\frac{d\theta_i}{dt} = \sum_j k_{ij}\theta_j(t) - \sum_i k_{ji}\theta_i(t)$$

where the rate constants k_{ij} are given by the Arrhenius equation $k_{ij} = Ae^{-\frac{\Delta G_a^{ij}}{k_B T}}$. ΔG_a^{ij} is the activation energy as was calculated from DFT simulations on Cu(100),[7] k_B is the Boltzmann constant, A is prefactor, around 10^{-13} s^{-1}.

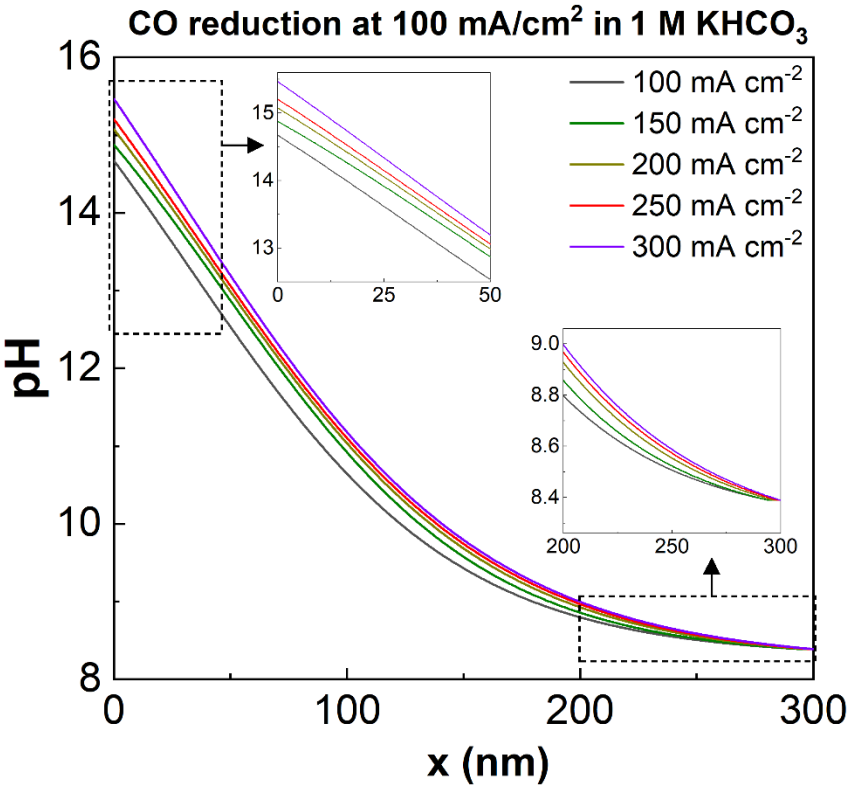

Figure S8. Calculated pH profiles for CO reduction in 1 M $KHCO_3$ at various current densities (x=0, surface pH; x> 0, local pH gradient near the surface).

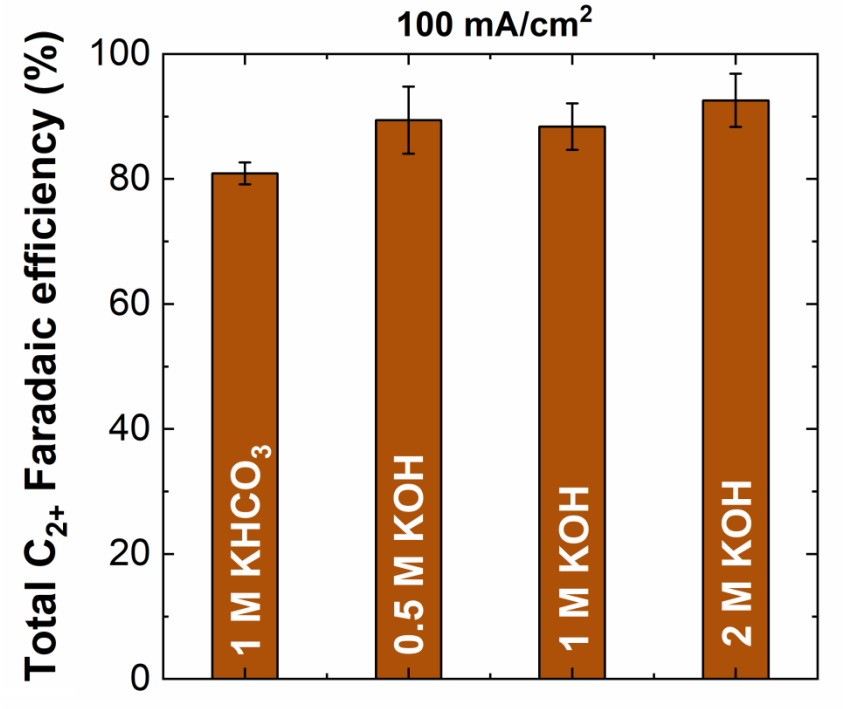

Figure S9. Faradaic efficiency for total C_{2+} products (including C_2H_4, acetate, acetaldehyde, ethanol and n-propanol) formed in CO reduction electrolysis at 100 mA/cm^2 in various pH electrolyte.

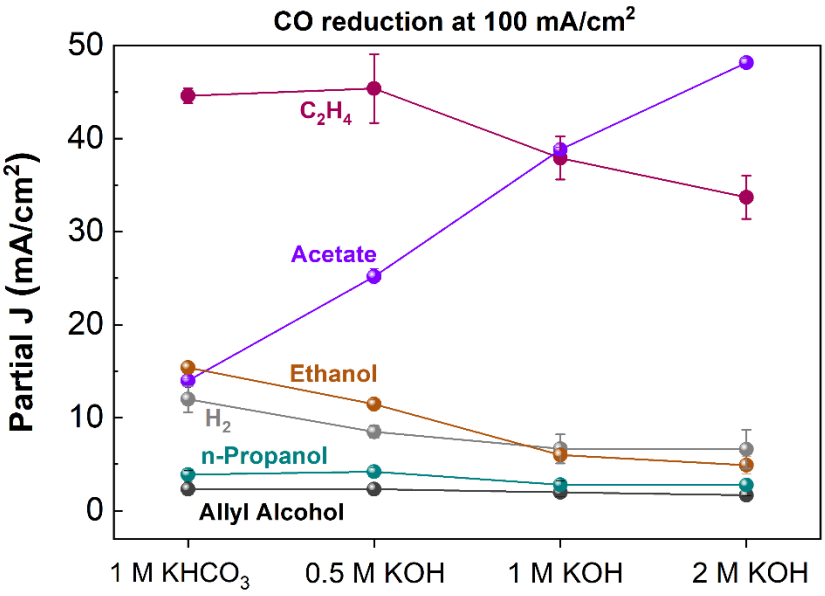

Figure S10. Partial current density of C_{2+} products in different pH electrolyte.

Electrolyte pH measurements

The bulk pH of the catholyte can influence the catalytic performance of CO reduction, thus we monitored pH of the electrolyte using a pH meter (pH 110, VWR) over the course of the CO reduction electrolysis. The temperature-compensation was performed via a temperature sensor that is coupled with the pH meter. In addition, a standard pH 7 buffer and a standard pH 10 buffer were utilized to calibrate the pH meter before the detection.

In addition, we also measured the anolyte pH over CO electrolysis. We found that the anolyte pH only had a slight variation after 3 h CO reduction electrolysis at 100 mA/cm^2 when using 1 M $KHCO_3$, 1 M KOH and 2 M KOH, respectively.

Applied potentials on the cathode

The solution resistance (Rs) was determined using potentiostatic electrochemical impedance spectroscopy (PEIS) in the GDE-type flow electrolyzers. A detailed procedure of PEIS was described in our previous work.[3] In this work, IR-corrected potentials were shown in the below Tables based on Rs determined by PEIS.

Table S6. IR-corrected potentials in 1 M $KHCO_3$.

Current (mA/cm^2)	Corrected V vs. SHE
50	-1.36
100	-1.42
150	-1.58
200	-1.70
250	-1.76
300	-1.80

Table S7. IR-corrected potentials at 100 mA/cm^2 in different electrolyte.

Electrolyte	Corrected V vs. SHE
1 M $KHCO_3$.	-1.42
0.5 M KOH	-1.44
1 M KOH	-1.44
2 M KOH	-1.47

Table S8. IR-corrected potentials as a function of CO concentration at a constant current density of 100 mA/cm^2 in 1 M KOH.

CO concentration	Corrected V vs. SHE
100%	-1.44
50%	-1.47
20%	-1.51
10%	-1.54
5%	-1.56

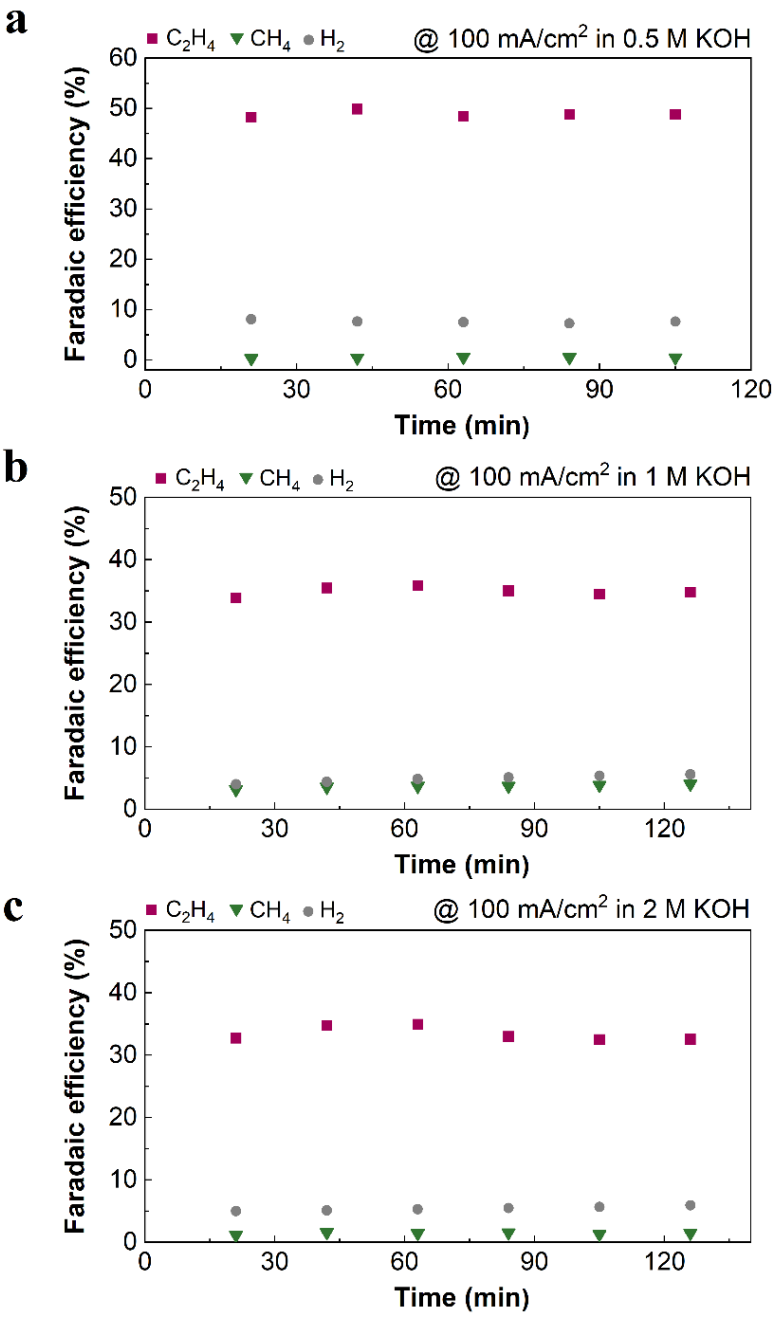

Figure S11. Catalytic selectivity of gas products on Cu catalysts for the electroreduction of CO in 0.5 M KOH (a), 1 M KOH (b) and 2 M KOH (c) at 100 mA/cm^2, respectively.

Table S9. Faradic efficiencies for all detected products in 1 M $KHCO_3$, 0.5 M KOH, 1 M KOH and 2 M KOH at 100 mA/cm^2 (due to only trace amounts of glycolaldehyde detected in this work, its faradaic efficiency is not added in Table S9).

electrolyte	Faradaic efficiency (%)								
	C_2H_4	CH_4	Acetate	Ethanol	n-Propanol	Allyl Alcohol	Acetaldehyde	H_2	Total
1 M $KHCO_3$	44.6	3.7	**14**	15.4	3.9	2.3	0.55	12	96.45
0.5 M KOH	45.4	1	**25.2**	11.5	4.2	2.3	0.53	8.5	98.63
1 M KOH	37.9	2.3	**38.8**	6.0	2.8	2.0	0.49	6.7	96.99
2 M KOH	33.7	1.2	**48.2**	4.9	2.8	1.7	0.68	6.6	99.78

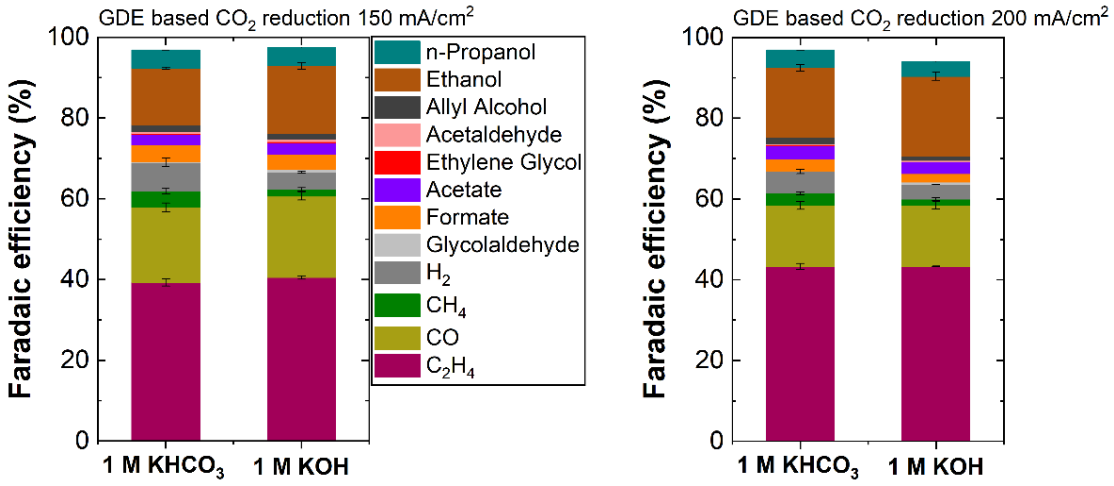

Figure S12. Comparison of the electrocatalytic CO_2 reduction performance in different electrolyte (no obvious discrepancy in acetate formation between 1 M $KHCO_3$ and 1 M KOH). This Figure S12 were adapted from the ref.3.

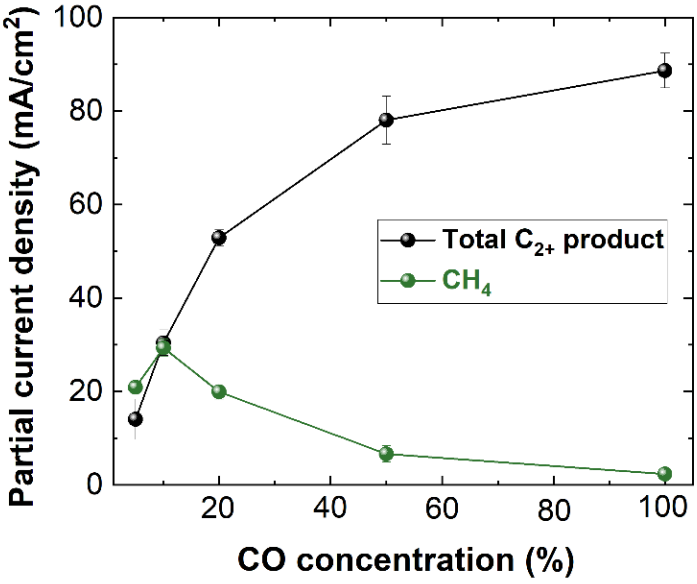

Figure S13. Comparison of partial current density of total C_{2+} and C_1 products in various CO concentration.

Difficulty in measuring ketene during CO electrolysis

We also tried to measure the ketene during CO electrolysis. Here, a silicon microchip-based electrochemistry/mass-spectrometry (EC-MS) system (Figure S14a) developed by our previous work[12] could offer the opportunity for real-time detection of the gaseous and volatile liquid product/intermediates of the electrochemical reaction. The CO reduction electrolysis was performed on polycrystalline Cu in CO-saturated 0.1 M K_2CO_3 electrolyte using this EC-MS system (it should be noted that KOH electrolyte cannot be used owing to the corrosion of silicon microchip). Although ketene should give a characteristic fragment $C_2H_2O^+$ at m/z 42, it is shared with acetaldehyde under the applied ionization energy of 22 eV. In addition, ketene is much less stable compared to acetaldehyde due to the adjacent C=C and C=O double bonds, thus making the calibration with a known concentration impossible. As shown in Figure S14b, m/z 42 signal was monitored as a function of applied potential. The results show that as the applied potential reduced from 0 V vs. RHE during CO reduction reaction in 0.1 M K_2CO_3, m/z 42 signal increased first and reached a vertex and dropped afterwards, accompanied by an elevated m/z 31 signal as the indicator of ethanol. This finding agrees well with the literature that acetaldehyde is the precursor of ethanol during electrochemical CO and CO_2 reduction. Thus, it is difficult to identify ketene even using the real-time detection. In addition, it should be noted that ketene is highly reactive, meaning that it would be very difficult to detect.

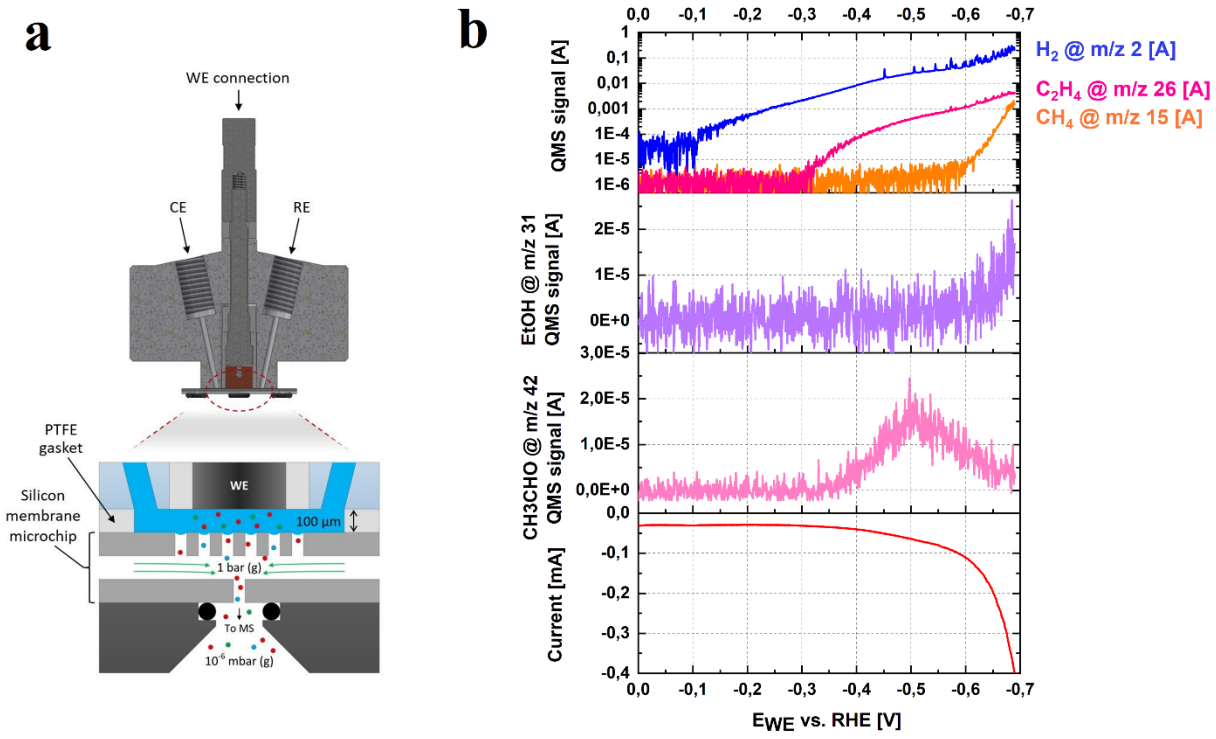

Figure S14. (a) Cross section of a cell-electrode assembly and membrane chip. (b) Electrochemical CO reduction on polycrystalline Cu in CO-saturated 0.1 M K_2CO_3 electrolyte using linear sweep voltammetry (LSV) at 0.2 mV/s. QMS signals are normalized by first extracting each of their own background signals before the electrolysis, then divided by the CO background signal (the highest) to eliminate influences of the electron multiplier on the signal intensity.

REFERENCES

[1] S. Nitopi, E. Bertheussen, S. B. Scott, X. Liu, A. K. Engstfeld, S. Horch, B. Seger, I. E. L. Stephens, K. Chan, C. Hahn, J. K. Nørskov, T. F. Jaramillo, I. Chorkendorff, *Chem. Rev.* **2019**, *119*, 7610–7672.

[2] K. P. Kuhl, T. Hatsukade, E. R. Cave, D. N. Abram, J. Kibsgaard, T. F. Jaramillo, *J. Am. Chem. Soc.* **2014**, *136*, 14107–14113.

[3] M. Ma, E. L. Clark, K. T. Therkildsen, S. Dalsgaard, I. Chorkendorff, B. Seger, *Energy Environ. Sci.* **2020**, *13*, 977–985.

[4] M. Ma, S. Kim, I. Chorkendorff, B. Seger, *Chem. Sci.* **2020**, *11*, 8854–8861.

[5] E. L. Clark, J. Resasco, A. Landers, J. Lin, L.-T. Chung, A. Walton, C. Hahn, T. F. Jaramillo, A. T. Bell, *ACS Catal.* **2018**, *8*, 6560–6570.

[6] S. J. Konopka, B. McDuffie, *Anal. Chem.* **1970**, *42*, 1741–1746.

[7] H. H. Heenen, G. Kastlunger, H. Shin, S. Overa, J. A. Gauthier, F. Jiao, K. Chan, ChemRXiv [preprint] **2021**, https://doi.org/10.33774/chemrxiv-2021-p3d4s

[8] J. Andraos, A. J. Kresge, *Can. J. Chem.* **2000**, 78, 508-515.

[9] E. L. Cussler, E. L. Cussler, Diffusion: mass transfer in fluid systems; Cambridge university press, **2009**.

[10] F. Gharagheizi, *Ind. Eng. Chem. Res.* **2012**, 51, 2797-2803.

[11] J. N. Hausmann, B. Traynor, R. J. Myers, M. Driess, P. W. Menezes, *ACS Energy Lett.* **2021**, *6*, 3567–3571.

[12] D. B. Trimarco, S. B. Scott, A. H. Thilsted, J. Y. Pan, T. Pedersen, O. Hansen, I. Chorkendorff, P. C. K. Vesborg, *Electrochim. Acta* **2018**, *268*, 520–530.